Photocatalytic Activity of Structured Mesoporous TiO_2 Materials

Mercedes Alvaro, Carmela Aprile, Miriam Benitez, Esther Carbonell, and Hermenegildo García*

Instituto de Tecnología Química CSIC-PV and Departamento de Química, Universidad Politécnica de Valencia, 46022 Valencia, Spain

Received: December 15, 2005; In Final Form: February 7, 2006

Starting from colloidal TiO_2 nanoparticles in combination with tetraethyl orthosilicate using neutral Pluronic or cationic cetyltrimethylammonium as templates, a series of structured mesoporous silicas has been obtained. The structure of the mesoporous titania was confirmed by isothermal gas adsorption, transmission electron microscopy, and X-ray diffraction. The pore diameter ranged between 3.8 and 10.9 nm, and the BET surface area varied from 99 to 584 $m^2\ g^{-1}$. The photocatalytic activity of these samples for the degradation of phenol in aqueous solution has been compared with that of standard P-25 TiO_2. Even though the activity of these new mesostructured materials is lower that those found for P-25 TiO_2, the turnover frequency of the photocatalytic activity (moles of phenol degraded per Ti atom present at initial reaction time) is much higher for the mesoporous titania, particularly with low titanium contents for those materials (mpTiO_2-5 and TiO_2-SBA15-5).

Introduction

Titanium dioxide is the most important semiconductor with large potential in photocatalysis, solar cells, photochromism, sensoring, and other applications in nanothecnology.[1−12] For many of these applications, the porosity, surface area, structure, crystal phase, particle size, and presence of dopants are factors that influence dramatically the activity and performance of titanium dioxide. While in the past decade and particularly after the seminal contribution describing the preparation of MCM materials there has been considerable progress in the preparation of mesoporous structured silicates,[13] progress in the synthesis of other metal oxides with analogous structure as that of porous silicas has been much more limited.[14−16] In contrast to the case of microporous solids and particularly titanosilicates such as a ETS-10,[17] one of the major problems in the preparation of the mesoporous metal oxides is their poor stability collapsing their structure very easily under mild conditions.[18−21] A novel strategy consists of using as building blocks for the preparation of a mesoporous material, not a monomeric molecular metal precursor, but colloidal nanoparticles adequately stabilized by ligands that after templation with surfactants in the usual way employed for mesoporous silicas will form part of the pore walls. Synthesis and calcination with particle sinterization and formation of covalent bonds between these nanoparticles finally produce a material that is considerably more robust and thermally more stable than those prepared analogously from molecular precursors. Very recently, related precedents to the present work have been published reporting the formation of mesoporous TiO_2 materials containing anatase nanocrystallites;[22,23] however, they used molecular precursor (titanium alcoxides) as the titania source to form these nanocrystallites, while here our approach is different. In the work reported here we used preformed TiO_2 nanoparticles as building blocks. The photochemical activity of films of mesoporous nanocrystalline anatase has been found to be larger than that of conventional unstructured anatase films.[24]

* To whom correspondence should be addressed. E-mail: hgarcia@qim.upv.es.

Results and Discussion

In this work we also describe the preparation of a mesoporous titanium dioxide material whose walls contain colloidal TiO_2 nanoparticles[25] embedded in silica domains having mesoporous periodic structure. In addition to the use of Pluronic triblock copolymer as a structure-directing agent to organize spatially the titanium dioxide nanoparticles, we also synthesized TiO_2 materials based on assembling nanoparticles using cetyltrimethylammonium bromide as surfactant. Since the surface affinity of TiO_2 particles for binding to polar species is well known, it was reasoned that hydrophilic Pluronic or quaternary ammonium ion could be a suitable templating agent for obtaining mesoporous titania from TiO_2 nanoparticles. Also, another feature of our synthetic methodology is the use of tetraethyl orthosilicate in the synthesis. Tetraethyl orthosilicate should co-condense during formation of the solid with the titania nanoparticles providing a more effective sintering of the TiO_2 nanoparticle building blocks without altering the band gap and photocatalytic efficiency of the solids, which would be basically determined by the TiO_2 nanoparticles. Scheme 1 shows the preparation route followed to obtain the mesoporous TiO_2 materials.

After the synthesis the structure-directing agent was removed from the solids by either calcination or solid−liquid extraction. When the samples were submitted to solid−liquid extraction, combustion chemical analyses of carbon and nitrogen reveal the complete absence of organic material.

The structure of the mesoporous titania materials was confirmed by isothermal gas adsorption, transmission electron microscopy, and X-ray diffraction. The pore diameter ranged between 3.8 and 10.9 nm**,** and the BET surface area varied between 99 and 584 $m^2\ g^{-1}$. The list of materials based on TiO_2 and the most relevant analytical and porosity data are given in Table 1.

10.1021/jp0573240 CCC: $33.50
Published on Web 03/09/2006

SCHEME 1: General Procedure Used for the Synthesis of Mesoporous Materials

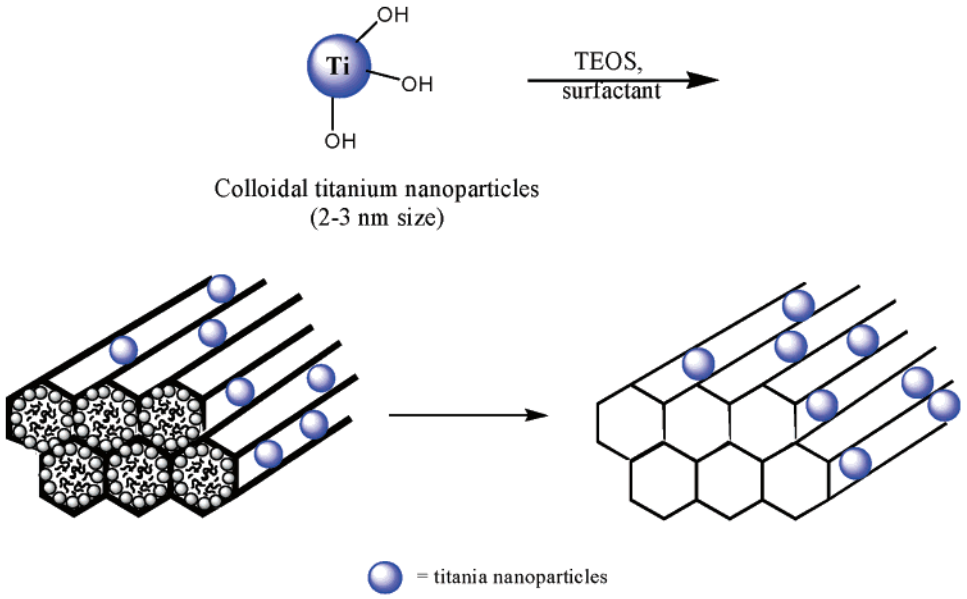

TABLE 1: Synthesis Procedure, Composition, and Porosity of the Mesoporous Titania Prepared in This Work

	synthesis conditions	Ti/TEOS content (wt %)	pore size (Å)	BET surface area (m^2/g)
TiO_2SBA15-5	as SBA15	5/95	38	584
TiO_2SBA15-50		50/50	46	388
TiO_2SBA15-100		99/1	109	115
mpTiO_2-5	as MCM-41	5/95	27	518
mpTiO_2-50		50/50	31	238
mpTiO_2-100		99/1	86	99
P25-TiO_2	commercial	100	*a*	45

[a] Amorphous, unstructured material.

The periodic mesoporous structure of the samples was clearly revealed by TEM. Figure 1 shows two representative images obtained for these mp-TiO_2 samples.

It is known that the photocatalytic activity of TiO_2 materials strongly depends on the relative anatase content. Raman spectroscopy can be used to distinguish between anatase (139, 389, 508, 634 cm^{-1}) and rutile (268, 400, 601 cm^{-1}) phases of TiO_2.[26] In our case, the crystal phase of the TiO_2 nanoparticles constituting the materials was determined for the synthesized and calcined samples. Figure 2 shows two characteristic Raman spectra representative for the samples. In general, they match very well with those expected for the anatase phase, even increasing the resolution and sharpness of the peaks for those samples submitted to calcination.

Diffuse reflectance UV−vis spectroscopy was used to determine the band gap of the structured mesoporous titania. From the onset of the absorption band it was estimated that the band gap of our samples is about 3.2 eV. This value is very similar to that reported for P-25 TiO_2 standard and is in good agreement with the fact that the original colloidal TiO_2 nanoparticles used as building blocks for the preparation of the mesoporous samples exhibit very similar diffuse reflectance UV−vis and band gap. It is interesting to comment that in contrast to related precedents where titania−silica mixed oxide has an increased band gap compared to the pure titania,[27,28] our samples prepared by titanium nanoparticles co-condensed with tetraethyl orthosilicate do not show this band gap increase. The reason for this is that in our sample the absorption band and band gap are intrinsically inherent to the TiO_2 nanoparticles and are not altered by the presence of silica domains in the solid, while in related work[29] there is really a co-condensation with the predominant formation of Si−O−Ti bonds corresponding truly to a mixed oxide. In our case there are domains in the material corresponding essentially to pure TiO_2. It is pertinent to comment that the photocatalytic activity of mixed silicon−titanium oxide was found to be significantly lower than that of P25 standard.

Comparing the diffuse reflectance UV−vis spectra of the samples before and after removal of the template it was observed that when the template was removed by solid−liquid extraction there were minor but reliable red shifts. Notably, these red shifts were much larger and significant, leading to variations of about 0.1 eV, when the structure directing agent was removed by air calcination under 400 °C. These spectral changes must be related to sintering and growth of the titania nanoparticles upon template

Figure 1. Selected TEM images showing the channel morphology and pore opening of mpTiO_2-100.

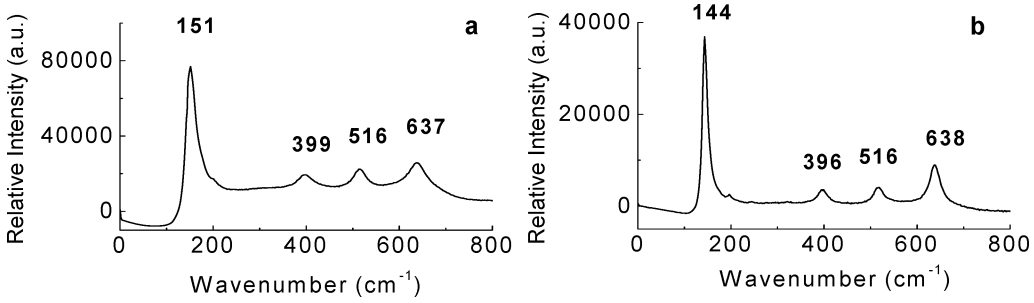

Figure 2. Raman spectra of calcined TiO_2SBA15-50 (a) and mpTiO_2-100 (b).

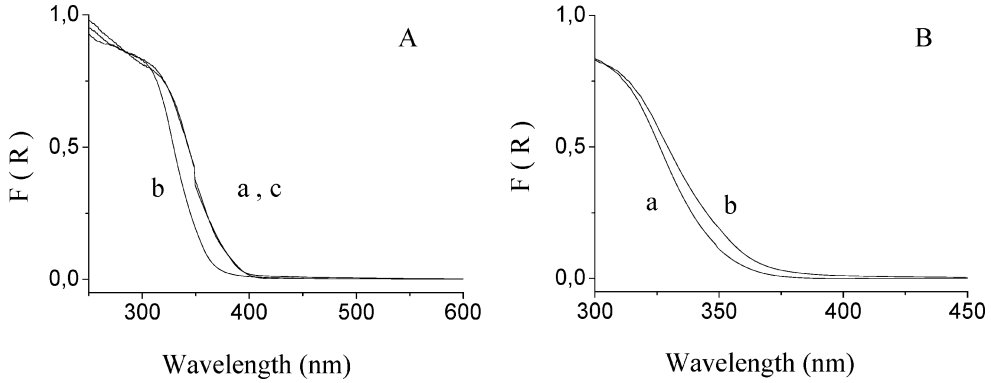

Figure 3. Diffuse reflectance UV−vis (plotted as the Kubelka−Munk function of the reflectance) spectra of (A) P25 (a), mpTiO_2-100 (b), TiO_2-SBA15−100 (c) and (B) mpTiO_2-100 (a) and mpTiO_2-100cal (b).

removal, indicating a restructuring of the material, which is more important when the method used for templated removal is calcination at high temperature.

The photocatalytic activity of the structured mesoporous titania samples was assessed for degradation of phenol in water.[30,31] In preliminary tests solvent-extracted mesoporous titania showed lower activity than the calcined ones. Thus, all the mesoporous materials tested for catalytic activity were previously calcined at 400 °C. As already commented, this thermal treatment increases the anatase-like phase of the material. In these photocatalytic tests the percentage of phenol disappearance from the aqueous solution is the magnitude being measured.[32] The two main parameters used to rank the relative photocatalytic activity of the solids have been the initial degradation rate (r_0) and the final degradation percentage after 3 h of irradiation. The reaction was carried out at room temperature using Pyrex-filtered light from a 125 W medium-pressure mercury lamp under aerobic conditions and continuous magnetic stirring. Blank controls showed that the phenol concentration remains constant when the irradiation is carried out under identical conditions but in the absence of any photocatalyst. The course of the reaction was followed by analyzing the phenol present in the solution and solid phase. r_0 was estimated from the slope at zero time of the time-conversion plot.

To obtain photocatalytic activity data valid for comparing the relative efficiency of different photocatalysts, one must first determine an adequate substrate−photocatalyst weight ratio.[33,34] In principle, upon increasing the amount of catalyst for a given weight of phenol, r_0 should increase linearly until a plateau is reached. In this regime further increase in the amount of photocatalyst used in the experiment does not lead to any further increase of r_0. This is due to the fact most of the photons entering into the suspension are already absorbed by the photocatalyst and further additional photocatalyst does not lead to an increase in either the number of photons adsorbed or the number of phenol molecules being degraded; therefore, r_0 remains constant.

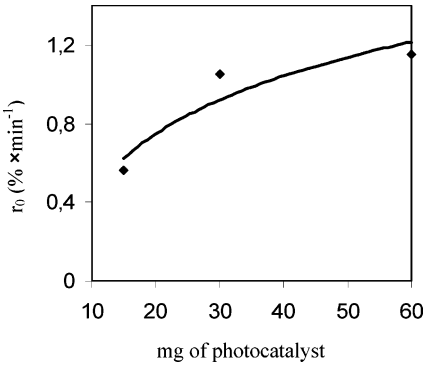

Figure 4. Plot of the initial disappearance (r_0) for the photocatalytic degradation of phenol (40 ppm) in water (20 ml) in the presence of different amounts of mpTiO_2-100.

Considering this typical behavior of r_0 versus the amount of photocatalyst, valid comparisons of the photocatalytic activity for different TiO_2 samples should be measured out of the saturation plateau but as close as possible to the maximum r_0. Otherwise those photocatalysts with different activity could exhibit the same r_0 simply due to saturation of the system. Figure 4 shows the plot of r_0 versus the amount of photocatalyst present in the suspension for the mpTiO_2-100 sample. mpTiO_2-100 is a solid with MCM-41 structure constituted almost exclusively by TiO_2 particles and is taken as reference sample for the rest of our structured mesoporous titania. From this plot we selected 30 mg of photocatalyst to perform the degradation of 20 mL of an aqueous solution containing 40 ppm of phenol. Throughout this work we maintained this substrate-to-photocatalyst ratio to compare the performance of the solid samples.

The photocatalytic data for the degradation of phenol in aqueous solution for each of the photocatalysts under selected experimental conditions are presented in Table 2. P-25 has been frequently used as a reference sample to compare the relative efficiency of any other titania sample. On the other hand, mesoporous MCM-41 silica not containing titanium was taken

TABLE 2: Photocatalytic Activity Measured as Initial Reaction Rate (r_0) and Final Degradation at 3 h of the Series of Mesoporous Titania (30 mg) for the Degradation of Phenol (40 ppm) in Water (20 mL) under Aerobic Conditions though Pyrex

photocatalyst	r_o (% min^{-1})	final degradation (%)	TOF [r_0(Ti content)$^{-1}$]
$mpTiO_2$-5	0.47	42	24.74
$mpTiO_2$-50	0.65	62	3.47
$mpTiO_2$-100	1.05	83	2.84
TiO_2SBA15-5	0.68	50	37.79
TiO_2SBA15-50	0.80	52	4.27
TiO_2SBA15-100	0.35	40	0.93
P-25	4.01	100	10.69
MCM-41	0.1	9	

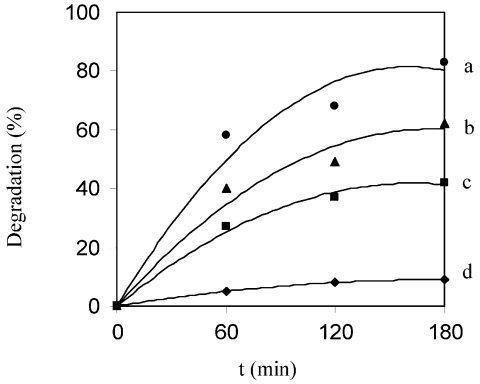

Figure 5. Percentage of photocatalytic degradation of phenol in aqueous solutions (40 ppm, 20 mL) in the presence of 30 mg of photocatalysts: (a) $mpTiO_2$-100, (b) $mpTiO_2$-50, (c) $mpTiO_2$-5, (d) blank using MCM-41.

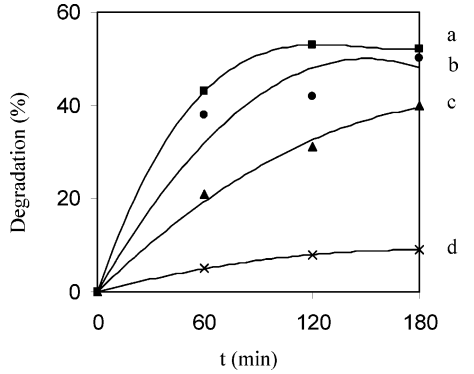

Figure 6. Percentage of photocatalytic phenol degradation (40 ppm, 20 mL) in the presence of 30 mg of photocatalysts: (a) TiO_2SBA15-50, (b) TiO_2SBA15-5, (c) TiO_2SBA15-100, (d) MCM-41 taken as a blank.

as a blank since very low photocatalytic activity is expected for this sample. Thus, as expected, upon irradiation of phenol (40 ppm in 20 mL) in the presence of MCM-41 (30 mg) only 9% of the starting amount was not recovered. This minor disappearance of phenol can be due to a combination of different factors, including direct photochemical degradation, photocatalytic degradation by MCM-41, and incomplete recovery of adsorbed phenol from the solid. This gives an indication of the relative efficiency of titania content photocatalyst.

The time-conversion plots for the disappearance of phenol in the presence of the series of photocatalysts are presented in Figures 5 and 6. Each data point in these plots corresponds to an independent experiment that was stopped at the required time and analyzed to determine the phenol content of the solution and solid. In the case of the $mpTiO_2$ series the photocatalytic activity (both the initial reaction rate and the final conversion) increases with the titanium content. This effect is, however, not observed for the SBA-15 series, for which there is a maximum of the photocatalytic activity as a function of TiO_2 content. The difference in activity between titanium-containing mesoporous materials with either MCM-41 or SBA-15 structure should reflect the influence of a combination of factors including surface area, porosity, particle size, and pore wall width that are different from MCM-41 and SBA-15.

From these activity data the following conclusions about the influence of analytical and structural parameters of the TiO_2-containing material on the photocatalytic activity can be obtained: (i) MCM-41-like synthesis gives materials with higher photocatalytic activity than those synthesized through a SBA-15-like procedure; (ii) the increase of the photocatalytic activity with the titanium content is not linear, samples with low titanium content exhibiting significantly higher turnover frequencies than those others with higher Ti content; (iii) the presence of silica domains does not interfere with the photocatalytic activity of the materials; (iv) using the same weight of photocatalyst the photocatalytic activity of P-25 is higher than that of mesoporous structured materials. The last conclusion about the relative photocatalytic activity of P-25 and mesoporous material is somehow disguised by the fact that according to the thermogravimetric profiles hydrophilic $mpTiO_2$ materials contain about 30% of weight in water. On the other hand, if the turnover frequency, i.e., mmoles of phenol degraded divided by the titanium content of the photocatalyst, is the factor being considered rather than r_0 or the final degradation, then the mesoporous TiO_2SBA15-5 and $mpTiO_2$-5 materials exhibit higher photocatalytic activity than P-25 (see Table 2).

TOF values are commonly used in catalysis to assess the average intrinsic activity per site. The fact that TOF values of mesoporous materials are higher than that of P-25 indicates that although the overall activity of mesoporous titania is lower, the intrinsic activity of each titanium atom in mesoporous titania is higher. As the titanium content of the mesoporous material increases, it may be that not all of the titanium dioxide particles are accessible to the photodegradable substrate. Then, the turnover frequency decreases and the activity of isolated not organized TiO_2 particles would be higher with regard to the relationship between TOF and final conversion. It is obvious that materials with lower initial activity values must require longer irradiation times to achieve similar values of final conversion.

In conclusion, periodic mesoporous titania photocatalysts containing silica domains have been synthesized starting from TiO_2 nanoparticles as building blocks. Their photocatalytic activity has been tested using phenol as a probe. Mesoporous titania with low titania content exhibits higher TOF values than that of P-25, which is due to the large surface area of the mesoporous material. Since our material is not really a mixed oxide but is constituted of TiO_2 nanoparticles, the existence of silica domains in other parts of the solids does not play any detrimental role on the photocatalytic performance.

Experimental Section

Combustion chemical analyses to determine the residual organic content were performed in a FISONS CHNOS analyzer. Powder X-ray diffraction patterns were obtained using a Phillips X'PERT diffractometer using filtered Cu Kα radiation. FT-IR spectra were recorded at room temperature with a Nicolet 710 spectrophotometer. Diffuse reflectance UV−vis spectroscopy was performed using a Cary 5G adapted with a praying mantis

accessory and using $BaSO_4$ as the standard. TEM experiments were carried out using a Philips CM300 FEG system with an operating voltage of 100 kV. Raman measurements (Renishaw inVia Raman Microscope) were carried out at room temperature with the 514.5 nm line of an Ar ion laser as the excitation source.

Synthesis of mpTiO_2 Material. In a typical procedure CTABr was added to a solution of NH_4OH and deionized water and the solution was stirred for 30 min in a closed polyethylene bottle to form a homogeneous solution. To that solution nanostructured particles of TiO_2 suspended in ethanol (20 mL) and the appropriate amount of TEOS dissolved in ethanol (5 mL) were mixed and added slowly to the CTABr solution at 50 °C for 2 h. TiO_2 nanoparticles were prepared by acid digestion of $Ti(O^iPr)_4$ in aqueous solution as previously reported.[25] Their nanometric particle size was determined by TEM. The molar ratio of the materials was: 1.00*X*:0.12CTABr: 8.0NH_3 (20%):114H_2O, where *X* corresponds to the sum of the Ti and Si atoms. Samples with varying Ti/(Ti + Si) ratio from 5 to 99 were prepared. The mixture was stirred at 50 °C for 1 h. Then the resulting gel was heated at 100 °C in static conditions for 4 days. The solid obtained was washed thoroughly with water and ethanol and dried at 100 °C for 3 h. The structure-directing agent was removed by calcination using the following temperature program: room temperature, 2 °C × min^{-1}, 400 °C for 5 h. Initially the sample was purged with nitrogen (1 mL min^{-1}), and after the first 5 h the flow was gradually replaced with air to complete surfactant combustion.

Synthesis of TiO_2SBA15 Materials. SBA-15 powder was prepared using the triblock copolymer, $EO_{20}PO_{70}EO_{20}$ (Pluronic P123). In a typical synthesis 3.46 g of Pluronic P123 was dissolved in 21.6 g of deionized water and 4.5 g of concentrated HCl (35%). To this mixture 42.9, 21.45, or 0.02 g of sodium silicate (5 wt % SiO_2 diluted from 25 wt %) and 0.125 (∼5.5 wt %), 1.072 (∼50 wt %), or 2.145 g (99 wt %) of nanoparticles of TiO_2[25] were quickly added under vigorous stirring at 35 °C. The weight ratio of the materials was 1.00*X*:1.60Pluronic P123: 2.1HCl (35%):10H_2O, where *X* corresponds to the sum of Ti and Si atoms. The mixture was stirred at 35 °C for 24 h and subsequently heated for 24 h at 100 °C under static conditions. The solid product was then filtered and dried at 100 °C. The structure-directing agent was removed by calcination.

Photocatalytic Tests. Photocatalytic tests were carried out stirring an air-saturated aqueous suspension (20 mL) of phenol (40 ppm) in the presence of photocatalyst (30 mg) in the open air at room temperature. The suspension was stirred for at least 10 min in the dark before irradiation. The samples were placed in a series of independent Pyrex test tubes (25 mL capacity), each provided with a magnetic stirring bar. The test tubes were placed in a thermostated water bath around a water-refrigerated Pyrex well containing a 125 W medium-pressure Hg lamp. The course of the irradiation was followed by taking each test tube at the required reaction time and analyzing the supernatant aqueous solution as well as the products retained in the solid. To recover the products from the solids they were extracted by sonicating the powder after redispersing in 3 mL of freshwater. The combined extracts (supernatant plus products recovered from the solid) were analyzed by reverse-phase HPLC (Suprasil column, diode array detector monitoring at 254 nm).

References and Notes

(1) Arshak, A.; Arshak, K.; Morris, D.; Korostynska, O.; Jafer, E. *Sens. Actuators, A* **2005**, *A122*, 242.

(2) Bossmann, S. H.; Goeb, S.; Siegenthaler, T.; Braun, A. M.; Ranjit, K. T.; Willner, I. *Fresenius' J. Anal. Chem.* **2001**, *371*, 621.

(3) Bossmann, S. H.; Jockusch, S.; Schwarz, P.; Baumeister, B.; Goeb, S.; Schnabel, C.; Payawan, L., Jr.; Pokhrel, M. R.; Woerner, M.; Braun, A. M.; Turro, N. J. *Photochem. Photobiol. Sci.* **2003**, *2*, 477.

(4) Bossmann, S. H.; Shahin, N.; Le Thanh, H.; Bonfill, A.; Worner, M.; Braun, A. M. *ChemPhysChem* **2002**, *3*, 401.

(5) He, T.; Yao, J.-N. *Res. Chem. Intermed.* **2004**, *30*, 459.

(6) Gyoergy, E.; Socol, G.; Axente, E.; Mihailescu, I. N.; Ducu, C.; Ciuca, S. *Appl. Surf. Sci.* **2005**, *247*, 429.

(7) Mihi, A.; Miguez, H. *J. Phys. Chem. B* **2005**, *109*, 15968.

(8) Wang, Y.; Jiang, X.; Xia, Y. *J. Am. Chem. Soc.* **2003**, *125*, 16176.

(9) Vione, D.; Minero, C.; Maurino, V.; Carlotti, M. E.; Picatonotto, T.; Pelizzetti, E. *Appl. Catal. B* **2005**, *58*, 79.

(10) Calza, P.; Medana, C.; Baiocchi, C.; Pelizzetti, E. *Appl. Catal. B* **2004**, *52*, 267.

(11) Calza, P.; Pelizzetti, E. *Pure Appl. Chem.* **2001**, *73*, 1839.

(12) Tsoukleris, D. S.; Arabatzis, I. M.; Chatzivasiloglou, E.; Kontos, A. I.; Belessi, V.; Bernard, M. C.; Falaras, P. *Sol. Energy* **2005**, *79*, 422.

(13) Vartuli, J. C.; Kresge, C. T.; Roth, W. J.; McCullen, S. B.; Beck, J. S.; Schmitt, K. D.; Leonowicz, M. E.; Lutner, J. D.; Sheppard, E. W. *Adv. Catal. Nanostruct. Mater.* **1996**, 1.

(14) Martin, M. E.; Narske, R. M.; Klabunde, K. J. *Microporous Mesoporous Mater.* **2005**, *83*, 47.

(15) Pinnavaia, T. J.; Kim, S. S.; Zhang, Z.; Liu, Y. *Stud Surf. Sci. Catal.* **2004**, *154A*, 14.

(16) Yokoi, T.; Yoshitake, H.; Tatsumi, T. *Chem. Mater.* **2003**, *15*, 4536.

(17) Xamena, F. X.; Calza, P.; Lamberti, C.; Prestipino, C.; Damin, A.; Bordiga, S.; Pellizeti, E.; Zecchina, A. *J. Am. Chem. Soc.* **2003**, *125* (8), 2264.

(18) Brezesinski, T.; Smarsly, B.; Iimura, K.-i.; Grosso, D.; Boissiere, C.; Amenitsch, H.; Antonietti, M.; Sanchez, C. *Small* **2005**, *1*, 889.

(19) Grosso, D.; Boissiere, C.; Smarsly, B.; Brezesinski, T.; Pinna, N.; Albouy, P. A.; Amenitsch, H.; Antonietti, M.; Sanchez, C. *Nat. Mater.* **2004**, *3*, 787.

(20) Mamak, M.; Metraux, G. S.; Petrov, S.; Coombs, N.; Ozin, G. A.; Green, M. A. *J. Am. Chem. Soc.* **2003**, *125*, 5161.

(21) Soten, I.; Ozin, G. A. *Supramol. Org. Mater. Des.* **2002**, 34.

(22) Ostomel, T. A.; Stucky, G. D. *Chem. Commun.* **2004**, *8*, 1016.

(23) Bartl, M. H.; Puls, S. P.; Tang, J.; Lichtenegger, H. C.; Stucky, G. D. *Angew. Chem., Int. Ed.* **2004**, *43*, 3037.

(24) Bosc, F.; Ayral, A.; Albouy, P.-A.; Guizard, C. *Chem. Mater.* **2003**, *15*, 2463.

(25) Addamo, M.; Augugliaro, V.; Di Paola, A.; Garcia-Lopez, E.; Loddo, V.; Marci, G.; Molinari, R.; Palmisano, L.; Schiavello, M. *J. Phys. Chem. B* **2004**, *108*, 3303.

(26) Cassiers, K.; Linssen, T.; Mathieu, M.; Bai, Y. Q.; Zhu, H. Y.; Cool, P.; Vansant, E. F. *J. Phys. Chem. B* **2004**, *108*, 3713.

(27) Anderson, C.; Bard, A. J. *J. Phys. Chem. B* **1997**, *101*, 2611.

(28) Yang, Q.; Xie, C.; Xu, Z.; Gao, Z.; Li, Z.; Wang, D.; Du, Y. *J. Mol. Catal. A* **2005**, *239*, 144.

(29) Gaertner, M.; Dremov, V.; Mueller, P.; Kisch, H. *ChemPhysChem* **2005**, *6*, 714.

(30) Hidaka, H.; Honjo, H.; Horikoshi, S.; Serpone, N. *New J. Chem.* **2003**, *27*, 1371.

(31) Serpone, N.; Terzian, R.; Lawless, D.; Pelletier, A.-M.; Minero, C.; Pelizzetti, E. *Aquat. Surf. Photochem.* **1994**, 387.

(32) Alvaro, M.; Carbonell, E.; Fornes, V.; Garcia, H. *New J. Chem.* **2004**, *28*, 631.

(33) Salinaro, A.; Serpone, N. *Pure Appl. Chem.* **1999**, *71* (2), 303.

(34) Emeline, A. V.; Frolov, A. V.; Ryabchuk, V. K.; Serpone, N. *J. Phys. Chem. B* **2003**, *107* (29), 7109.